# Artemin promotes functional long-distance axonal regeneration to the brainstem after dorsal root crush

Laura Elisabeth Wong[a], Molly E. Gibson[a], H. Moore Arnold[b], Blake Pepinsky[c], and Eric Frank[a,1]

[a]Department of Integrated Physiology and Pathobiology, Tufts University School of Medicine, Boston, MA 02111; and [b]Neurology Research and [c]Chemical and Molecular Therapeutics, Biogen Idec, Inc., Cambridge, MA 02142

Edited by Nicholas Spitzer, University of California at San Diego, La Jolla, CA, and approved March 31, 2015 (received for review January 30, 2015)

**Recovery after a spinal cord injury often requires that axons restore synaptic connectivity with denervated targets several centimeters from the site of injury. Here we report that systemic artemin (ARTN) treatment promotes the regeneration of sensory axons to the brainstem after brachial dorsal root crush in adult rats. ARTN not only stimulates robust regeneration of large, myelinated sensory axons to the brainstem, but also promotes functional reinnervation of the appropriate target region, the cuneate nucleus. ARTN signals primarily through the RET tyrosine kinase, an interaction that requires the nonsignaling coreceptor GDNF family receptor (GFRα3). Previous studies reported limited GFRα3 expression on large sensory neurons, but our findings demonstrate that ARTN promotes robust regeneration of large, myelinated sensory afferents. Using a cell sorting technique, we demonstrate that GFRα3 expression is similar in myelinated and unmyelinated adult sensory neurons, suggesting that ARTN likely induces long-distance regeneration by binding GFRα3 and RET. Although ARTN is delivered for just 2 wk, regeneration to the brainstem requires more than 3 mo, suggesting that brief trophic support may initiate intrinsic growth programs that remain active until targets are reached. Given its ability to promote targeted functional regeneration to the brainstem, ARTN may represent a promising therapy for restoring sensory function after spinal cord injury.**

artemin | GFRα3 | regeneration | dorsal root crush | cuneate nucleus

Spinal cord (SC) injury results in permanent paresis and paralysis, owing in large part to the failure of axons to regenerate. In the adult SC, axons do not regenerate because of myelin- and injury-associated inhibitory barriers and a limited intrinsic regenerative ability (1). Although there has been some success in removing extrinsic barriers and providing neurotrophic factors to promote functional regeneration over short distances (2–4), meaningful functional recovery requires that damaged axons regenerate and reconnect with their original targets, often centimeters away from the lesion. Studies in which damaged sensory axons were induced to regenerate to the brainstem have failed to show reestablishment of synapses (5). These findings cast doubt on whether sensory axons can regenerate functionally to the brainstem.

Dorsal root (DR) crush provides a useful model for studying long-distance axon regeneration without affecting the architecture of the SC. Fine touch and proprioceptive neurons with cell bodies in the DR ganglion (DRG) provide monosynaptic input to neurons in the dorsal column nuclei. These neurons can be traced using transganglionic labeling methods and are easily studied electrophysiologically, making this an ideal injury model for investigating functional regeneration from the brachial SC to the brainstem.

Previous studies demonstrated that a 2-wk systemic treatment with the neurotrophic factor artemin (ARTN) promotes topographically specific regeneration of both myelinated and unmyelinated sensory axons into the SC at 1 mo after DR crush (3, 6). This results in persistent recovery of simple behavioral tasks and of electrophysiological function in the SC. In addition, Wang et al. (3) provided evidence that ARTN might promote sensory axon regeneration to the brainstem, although the extent, functionality, and mechanism of regeneration to distant targets remain unknown.

The major mechanism of ARTN action is via binding to a nonsignaling coreceptor, GDNF family receptor (GFRα3), and the RET receptor tyrosine kinase, forming a complex that activates intracellular signaling cascades (7). Earlier studies suggested that GFRα3 is expressed primarily in small sensory neurons, with limited expression in large neurons (8, 9); thus, how ARTN promotes robust regeneration of large sensory axons is unclear.

In this paper, we report that ARTN induces functional regeneration of myelinated sensory axons across several centimeters to the brainstem. Over several months after DR crush, sensory axons in ARTN-treated rats regenerate to the cuneate nucleus (CN), where they reestablish functional synapses. Given this evidence of large-fiber regeneration, we investigated whether myelinated sensory neurons express GFRα3. In contrast to earlier studies, we found that GFRα3 is expressed at comparable levels in myelinated and unmyelinated sensory neurons, providing a basis for the long-distance regeneration described here.

## Results

**Crushed Brachial Sensory Axons Regenerate to the Brainstem.** To test whether sensory axons regenerate to the CN, we performed a unilateral DR crush from from cervical level 5 (C5) through thoracic level 1 (T1) and treated rats with ARTN or vehicle. At 6 mo postlesion, we examined brainstem sections for the presence of regenerated axons peripherally labeled with fluorescent dextran. With intact roots, axon terminals in the CN of the brainstem were robustly labeled and tightly clustered (Fig. 1*A*). The DR crush interrupted all brachial sensory axons traveling to the brainstem, as demonstrated by the elimination of fluorescent puncta in the CN in vehicle-treated animals (Fig. 1*B*). Virtually no labeled axons were present in the SC of vehicle-treated animals at any time point examined (1.5, 3, and 6 mo after DR crush), consistent with the

### Significance

**Recovery after a spinal cord injury requires that axons regenerate and reconnect with their original targets. Here we report that after interruption of sensory axons in dorsal roots, systemic treatment with a naturally occurring growth factor, artemin (ARTN), promotes regeneration of these axons 3–4 cm away from their original target region in the brainstem, where they reestablish functional connections. In contrast to earlier studies, we also find that GDNF family receptor, a known receptor for ARTN, is expressed on both myelinated and unmyelinated sensory neurons, consistent with ARTN's ability to promote regeneration of large and small sensory neurons.**

Author contributions: L.E.W., M.E.G., and E.F. designed research; L.E.W. and M.E.G. performed research; L.E.W., H.M.A., and B.P. contributed new reagents/analytic tools; L.E.W., M.E.G., and E.F. analyzed data; and L.E.W. and E.F. wrote the paper.

Conflict of interest statement: H.M.A. and B.P. are full-time employees and stockholders of Biogen Idec, Inc. The other authors declare no conflict of interest.

This article is a PNAS Direct Submission.

[1]To whom correspondence should be addressed. Email: eric.frank@tufts.edu.

This article contains supporting information online at www.pnas.org/lookup/suppl/doi:10.1073/pnas.1502057112/-/DCSupplemental.

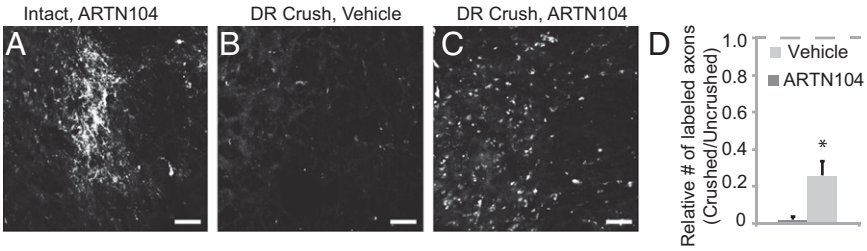


**Fig. 1.** Systemic ARTN104 promotes axon regeneration to the CN. (*A*–*C*) Representative cross-sections through the CN at 6 mo after DR crush. (*A*) On the intact side, numerous fluorescent puncta (cross-sections through peripherally labeled axons) were visualized in the CN. (*B*) After DR crush, virtually no puncta were seen in the CN of vehicle-treated rats. (*C*) With ARTN104 treatment, puncta were observed in the CN on the crushed side in a diffuse distribution. (Scale bars: 100 μm.) (*D*) Quantification of the puncta in the CN in vehicle-treated ($n = 5$) and ARTN104-treated ($n = 8$) animals, expressed as the ratio of puncta on the crushed side over puncta on the intact side in the same animal. With ARTN treatment, there was recovery to 25% of normal, a significant improvement over vehicle treatment. Error bars represent SEM. *$P < 0.05$.

fact that crushed sensory axons stop regenerating at the DR entry zone, the transitional zone between the peripheral nervous system and CNS (6, 10). In animals treated with systemic ARTN104, substantial numbers of labeled puncta in the ipsilateral CN were evident at 6 mo after DR crush (Fig. 1*C*), confirming that ARTN promotes long-distance regeneration. Puncta were located in approximately the same brainstem region as in uninjured animals, suggesting that ARTN promotes directed regeneration even over long distances (Fig. 1*C*). On average, there were ∼25% as many puncta as in the intact projections on the contralateral side, representing a significant improvement over vehicle treatment ($P = 0.04$) (Fig. 1*D*). Thus, systemic ARTN treatment promotes regeneration of crushed brachial sensory axons to the brainstem within 6 mo after DR crush.

**ARTN Restores Synaptic Inputs in the Brainstem.** We assessed the recovery of synaptic function in the brainstem through extracellular recordings from the CN in response to stimulation of the median and ulnar nerves. Most responses mediated by intact sensory axons have latencies of 0.9–1.3 ms and synaptic responses (quantified as the average response from 0.5 to 6.5 ms) of 250–400 μV (Fig. 2*A*). These field potentials (i.e., synaptic potentials) in brainstem neurons are evoked by activity in large-caliber myelinated sensory axons. The synaptic response was similar on the unlesioned side in ARTN104- and vehicle-treated animals. Synaptic potentials were abolished in all vehicle-treated animals tested (Fig. 2 *A* and *C*). In contrast, all animals treated with systemic ARTN104 showed recovery of synaptic function at 6 mo after DR crush (Fig. 2*A*). The ratio of the synaptic potential on the crushed side over the intact side was 0.23 ± 0.02 ($n = 8$), much greater than that in vehicle-treated animals (0.01 ± 0.006; $n = 5$; $P < 0.001$). Similar to previous findings in the SC (2, 3), synaptic potential latencies evoked by regenerating axons were longer than those evoked by unlesioned axons (2.2 ± 0.2 ms vs. 1.1 ± 0.1 ms; $n = 8$; $P < 0.001$) (Fig. 2*A*). These data are consistent with smaller-caliber regenerating axons (11).

To verify that the synaptic potentials originated from the injured DRs, DRs from C5–T1 were cut at the end of each electrophysiology session. This completely abolished the synaptic potentials in the brainstem and SC, indicating that the response is mediated through those roots. These data demonstrate that after DR crush and systemic ARTN treatment, regenerating brachial sensory axons reestablish functional synapses with targets in the CN, 3–4 cm from the lesion site, within 6 mo after the crush surgery.

**Restoration of Synaptic Input Requires a Long Recovery Time.** Our previous experiments indicated that a relatively short recovery time (∼1 mo) is required for local regeneration and restoration of synaptic input in the brachial spinal cord (2, 3). In contrast, regeneration to the brainstem should require significantly more time because of the greater distance axons must regenerate from the lesion.

To verify that the synaptic connections that we observed in the brainstem after DR crush did not originate from axons spared in the crush surgery, we assessed the synaptic response in the CN and SC in animals that recovered for 1.5, 3, or 6 mo after DR crush. Our initial experiments were carried out in animals treated with ARTN104, a truncated version of ARTN with nine N-terminal amino acids removed to reduce binding to heparan sulfate proteoglycans (12). Because of constraints on our supply of ARTN104, we conducted subsequent experiments using ARTN113, a longer form of ARTN containing 113 amino acids that we had used in previous studies (3, 6).

We first assessed whether ARTN113, like ARTN104, could restore synaptic input by recording brainstem and SC synaptic responses. With ARTN113 treatment, 50% of the animals (three of six) had recovered synaptic function in the SC and brainstem at 6 mo postlesion, in contrast to all eight animals treated with ARTN104. In the three animals in which synaptic input was reestablished, synaptic potential shape, size, and latency were similar to

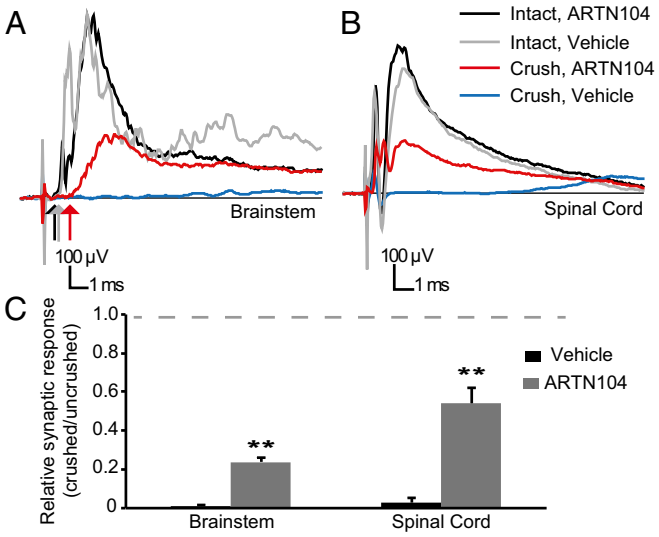


**Fig. 2.** ARTN104 treatment restores synaptic connectivity with the CN. (*A* and *B*) Representative field potentials recorded at 6 mo after DR crush in the CN (*A*) and SC (*B*) elicited by stimulation of the median and ulnar nerves. ARTN treatment did not affect the amplitude or latency (arrows) of synaptic potentials on the unlesioned side (black and gray). With ARTN treatment (red), a synaptic response with long latency (red arrow) was present in the CN and SC, indicating functional regeneration. There was no response in the SC or CN after DR crush in vehicle-treated animals (blue). (*C*) Quantification of the synaptic response recorded in all animals and normalized to the intact side (ARTN104, $n = 8$; vehicle, $n = 5$). The dashed line represents complete recovery. Error bars represent SEM. **$P < 0.001$.

NEUROSCIENCE

those in animals treated with ARTN104 (Figs. 2 and 3). A recovery period of only 1.5 or 3 mo was not sufficient to allow regeneration to the CN, however (Fig. 3*A*). In animals that had recovered for these short time periods, ARTN113 promoted restoration of synaptic connections in the SC in 6 of 8 animals, and the synaptic potentials were similar in shape, size and latency for all recovery times (Fig. 3 *B* and *D*). Despite synaptic activity in the SC, none of these animals had any synaptic response in the brainstem on the lesioned side (Fig. 3*A*). By 6 mo postlesion, synaptic function was reestablished in the CN to ~18% of normal, significantly greater than the regeneration at earlier time points ($P = 0.002$, ANOVA) (Fig. 3 *A* and *C*).

The foregoing data indicate that restoration of synaptic function takes significantly longer in the brainstem than in the SC, consistent with the distance over which that axons must regenerate. Because spared axons recover rapidly (11), the lack of response at 1.5 and 3 mo suggests that axons are unlikely to be spared after DR crush. In the three animals excluded from the study because of overly rapid behavioral recovery (suggestive of an incomplete DR crush; *Materials and Methods*), synaptic potential latencies and rise times were comparable to those on the uninjured side after only 1.5 mo (data not shown).

To further verify that long-distance regeneration is time-dependent, we counted puncta in the CN of ARTN113-treated rats that had recovered for 1.5, 3, and 6 mo postcrush and had synaptic recovery in the SC. No puncta were observed above background in the CN at 1.5 mo ($n = 2$) or 3 mo ($n = 3$), despite the presence of numerous labeled sensory axons in the dorsal horn of the brachial SC (Fig. 4). In contrast, numerous fluorescent puncta were present in the CN of ARTN113-treated animals at 6 mo postcrush ($n = 3$), a significant improvement over earlier time points ($P = 0.04$, ANOVA) (Fig. 4). In animals with functional regeneration, both ARTN113 and ARTN104 resulted in the recovery of 25–30% of the normal number of labeled terminals ipsilateral to the crush (Figs. 1*B* and 4*B*). These data confirm the expectation that long-distance regeneration to the CN takes significantly longer than regeneration to the brachial SC.

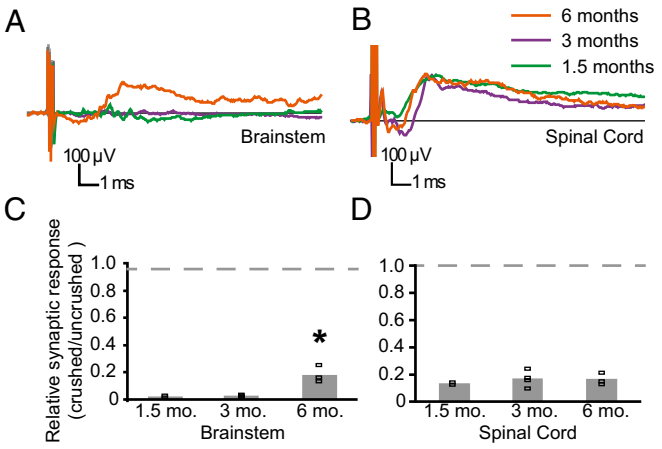


**Fig. 3.** Restoration of synaptic function to the CN requires significant time. (*A* and *B*) Representative field potentials recorded in the CN (*A*) and SC (*B*) on the crushed side in ARTN113-treated rats after 1.5, 3, and 6 mo of recovery. (*A*) A synaptic potential was present in the CN only in ARTN-treated rats at 6 mo recovery (orange). (*B*) There were no responses in the CN in rats recovering for 1.5 or 3 mo (green and purple, respectively) despite similar synaptic potentials in the SC at each time point; thus, the lack of response in the CN at early times is not related to the failure of ARTN113 to promote regeneration. (*C*) Quantification of the synaptic responses in the CN normalized to the intact side in ARTN113-treated rats (1.5 mo, $n = 2$; 3 mo, $n = 4$; 6 mo, $n = 3$), excluding 5 of 14 animals with no regeneration (*Results*). By 6-mo postlesion, ARTN113 promoted significant synaptic recovery. (*D*) Quantification of the synaptic responses in the SC in the same rats. Symbols depict synaptic responses for each animal. Bars indicate the average response. $^*P < 0.05$.

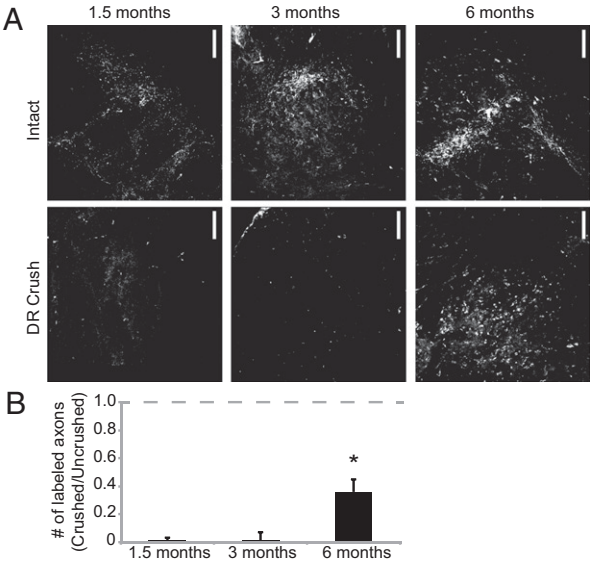


**Fig. 4.** More than 3 mo is required for axonal regeneration to the CN. (*A*) Representative cross-sections through the CN in ARTN113-treated animals at 1.5, 3, and 6 mo after DR crush. On the intact side, there were numerous puncta in the CN. At 1.5 and 3 mo postlesion, virtually no puncta were present in the CN on the crushed side, similar to vehicle-treated rats. By 6 mo postlesion, puncta were present in the CN on the crushed side, as observed with ARTN104 treatment. (*B*) Quantification of the fluorescent puncta in the CN, expressed as the ratio of puncta on the crushed side over those on the intact side (1.5 mo, $n = 2$; 3 mo, $n = 4$; 6 mo, $n = 3$). Error bars represent SEM. $^*P < 0.05$.

**GFRα3 Is Present in Both Myelinated and Unmyelinated Sensory Neurons.** Some previous studies have suggested that GFRα3, the high-affinity binding partner of ARTN, is expressed predominantly in small, unmyelinated sensory neurons, with limited to no expression in large, myelinated neurons (8, 9, 13, 14). Nevertheless, myelinated fibers regenerate after ARTN treatment, suggesting that GFRα3 may be more widely expressed than previously reported.

To assess GFRα3 expression in large, myelinated neurons, we stained sections of adult DRGs with antibodies to GFRα3 and either the neurofilament heavy chain (NF200), which identifies large sensory neurons, or calcitonin gene-related peptide (CGRP), which identifies a subpopulation of small sensory neurons (Fig. 5 *A* and *B*). As expected, the majority of $CGRP^+$ cells (92 ± 4%) expressed GFRα3 (Fig. 5*A*). Of note, a significant percentage of $NF200^+$ cells (84 ± 4%) also expressed $GFR\alpha^+$ (Fig. 5*B*), suggesting that the coreceptor is expressed in large-diameter neurons. Because our results differed from previous reports (8, 9, 13, 14), we were concerned that the commercially available GFRα3 antibody might bind nonspecifically.

To verify the specificity of GFRα3 immunolabeling, we immunostained DRG tissue from mice with a genetic deletion of GFRα3 and their heterozygous littermates (15). There was no GFRα3 immunoreactivity in $GFR\alpha3^{-/-}$ murine DRGs (Fig. S1*A*); in contrast, nearly all neurons expressed GFRα3 in $GFR\alpha3^{+/-}$ mice (Fig. S1*B*). These findings demonstrate that GFRα3 antibody binding is specific, and provides strong evidence that GFRα3 is expressed by both large and small DRG neurons.

To provide further support for GFRα3 expression in large sensory neurons, we developed a method to identify and physically separate large and small neurons so we could assess the expression of GFRα3 mRNA using quantitative PCR (qPCR). Populations of small and large neurons were identified by injecting peripheral nerves with wheat germ agglutinin conjugated to Alexa Fluor 647

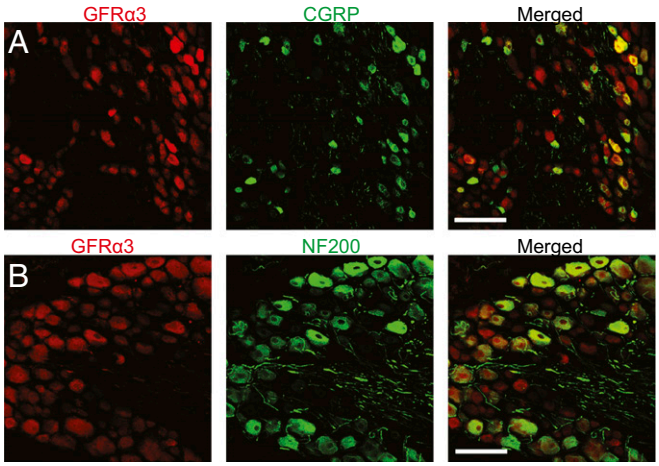


**Fig. 5.** GFRα3 immunoreactivity is present in both large and small sensory neurons in the DRGs of rats. (*A*) Representative DRG section stained with antibodies to GFRα3 (red) and CGRP (green), identifying a subset of small, unmyelinated neurons. 92 ± 4% of CGRP$^+$ cells express GFRα3. (*B*) Representative DRG section stained with antibodies to GFRα3 (red) and NF200 (green), labeling a subset of large, myelinated neurons. 84 ± 4% of NF200$^+$ cells express GFRα3. These data indicate that GFRα3 is expressed on both types of neurons. (Scale bars: 100 μm.)

(WGA-647), labeling a subpopulation of small sensory neurons, and cholera toxin B subunit conjugated to Alexa Fluor 488 (CTB-488), labeling large, myelinated sensory neurons (16, 17). As expected, few neurons were labeled with both neurotracers (Fig. 6 *A* and *B*), verifying that these neurotracers label distinct neuronal populations.

We confirmed the specificity by staining sections of prelabeled DRGs with NF200 and CGRP. More than 60% of CTB$^+$ neurons expressed NF200, whereas only 7% expressed CGRP (Fig. 6 *A*–*C*). When cells labeled with both CTB and WGA were excluded, only 3% of CTB$^+$ neurons expressed CGRP. In contrast, 48% of WGA$^+$ neurons expressed CGRP and 17% expressed NF200 (Fig. 6 *A*–*C*). Consistent with previous reports (16), CTB$^+$ cells are larger than WGA$^+$ cells (Fig. S2). These data confirm that labeling peripheral nerves with CTB and WGA is a suitable method for differentiating large and small DRG sensory neurons (16, 17). Dissociated sensory neurons prelabeled with WGA and CTB were sorted into separate fractions by fluorescence-activated cell sorting (FACS) (Fig. 6*D*). qPCR using the genes for GAPDH and HPRT as reference genes showed that relative levels of GFRα3 mRNA were similar in CTB$^+$ and WGA$^+$ neurons (Pfaffl ratio: for CTB$^+$, 1.03; for WGA$^+$, 1.09; $P = 0.82$). Both large and small sensory neurons express GFRα3 Given the presence of GFRα3 transcript and protein in both neuronal types, ARTN likely promotes regeneration via the canonical pathway involving high-affinity binding to GFRα3 and subsequent RET activation (18). We cannot rule out the possibility of alternative binding partners, however.

**GFRα3 Expression Decreases After DR Crush.** Previous studies indicated that GFRα3 is up-regulated after axonal injury (3, 8, 14). We assessed the effects of DR crush on GFRα3 gene expression using qPCR. In contrast to previous studies, we found that GFRα3 expression was decreased at 2 d after DR crush (Pffafl ratio: for intact neurons, 1.06; for DR crush neurons, 0.64; $P = 0.01$) (Fig. 7*A*). To determine whether this trend also occurred at the protein level, we measured changes in GFRα3 immunoreactivity in DRG neurons from rats subjected to unilateral DR crush. We found a significant decrease in mean pixel intensity in DRG neurons at 2 d after crush (32.0 ± 0.7, $n = 271$ cells from three animals) compared with DRG neurons from the intact side (46.4 ± 0.9, $n = 276$ cells from three animals) in the same animals (Fig. 7 *B* and *C*). Furthermore, no cells expressed high levels of GFRα3. This decrease in average immunoreactivity for GFRα3 protein was maintained for 12 d after crush (intact, 41.3 ± 0.8; crush, 34.3 ± 0.7; $P < 0.001$) (Fig. 7 *B* and *C*). These data indicate that GFRα3 expression decreases after DR crush.

## Discussion

Long-distance regeneration is required for restoration of function after SC injury. To date, regeneration in the SC has been limited to several millimeters, with no reestablishment of functional connectivity in many cases. Systemic ARTN treatment promotes the regeneration of crushed sensory axons from the brachial SC to the brainstem, a distance >3 cm in adult rats. This regeneration restores substantial synaptic connectivity with neurons in the CN at 6 mo after DR crush (Fig. 2). Although we are not aware of any behavioral tests for restoration of sensory input to the brainstem, simple reflexive behaviors are markedly improved with a 20% restoration of synaptic function in the SC (3). This suggests that the level of synaptic connectivity in the brainstem demonstrated here might be behaviorally relevant.

One concern about the DR crush model of spinal injury is that axons may be spared in the crush (11). Although no labeled axons or synaptic responses were observed in the SC of vehicle-treated animals (Figs. 1 and 2), ARTN might promote recovery of damaged sensory axons rather than regeneration of crushed axons. Several observations indicate that recovery was largely the result of regeneration. First, all animals underwent rigorous behavioral testing shortly after crush surgery, and the few animals that recovered the use of the ipsilateral forelimb in the first 2 wk after DR crush were excluded from the study. Second, the latency to the onset of synaptic activity was twice as long in postsynaptic neurons receiving input from crushed axons as in those receiving input

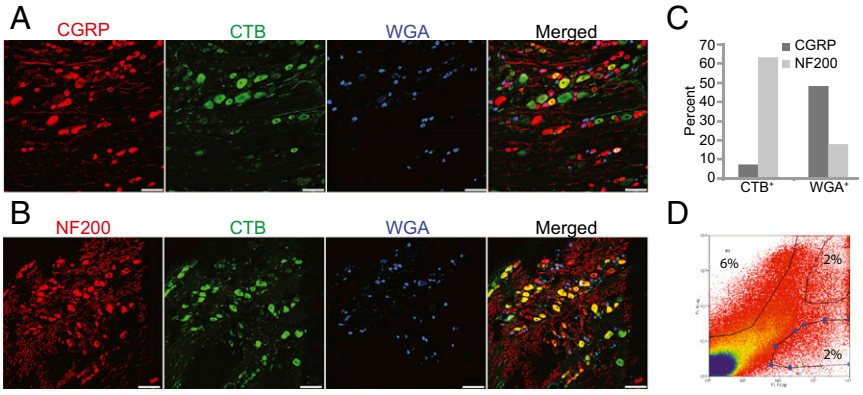


**Fig. 6.** WGA and CTB label distinct classes of DRG sensory neurons. (*A* and *B*) Representative sections through the DRG prelabeled with CTB-488 and WGA-647 and immunolabeled with an antibody to CGRP (*A*) or NF200 (*B*). (*C*) Quantification of the percentage of CTB$^+$ and WGA$^+$ cells labeled with NF200 and CGRP antibodies. Most CTB$^+$ neurons are large, myelinated neurons, whereas many WGA$^+$ neurons are small, nociceptive neurons. (*D*) FACS profiles of dissociated DRGs prelabeled with CTB and WGA. The percentages of neurons sorted in each condition are labeled in the gated areas. Gates were set to ensure collection of only strongly and singly labeled cells. (Scale bars: 100 μm.)

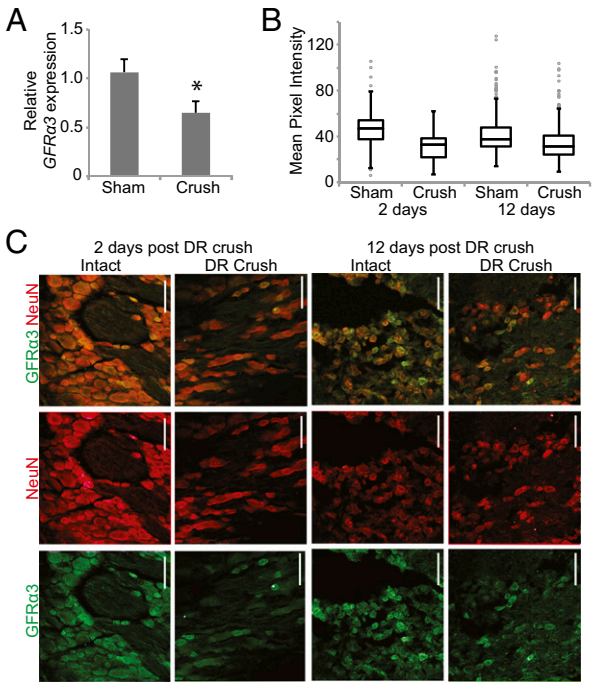


**Fig. 7.** GFRα3 expression decreases after DR crush injury. (*A*) Quantification of the relative ratio of GFRα3 mRNA expression in DRG neurons from the crushed or uncrushed side 2 d after injury, normalized to both *GAPDH* and *HPRT*. After DR crush, GFRα3 expression was decreased in sensory neurons. Error bars represent SEM. $*P < 0.05$. (*B*) Boxplots showing the mean pixel intensity of GFRα3 immunostaining in DRG neurons (2 d intact, $n = 276$; 2 d crush, $n = 271$; 12 d intact, $n = 400$; 12 d crush, $n = 403$). Outliers (>1.5 interquartile range) are depicted by gray circles. (*C*) Representative cross-sections through DRGs from rats with unilateral DR crush stained with antibodies to GFRα3 and NeuN (to identify neurons) used for the quantification in *B*. (Scale bars: 100 μm.)

from uninjured axons (Fig. 2*A*), consistent with a smaller caliber of regenerated axons (3, 11). Third, labeled axons and synaptic responses were present in the CN only after several months of recovery (Figs. 3 and 4). Spared axons recover over the course of days, not months (11); thus, if synaptic responses were the result of spared axons, then recovery in the CN would occur at the same time as in the SC. The most parsimonious explanation for the substantial time to the appearance of labeled axons in the CN is that axons regenerate from the site of injury in the DR. These data provide strong evidence that ARTN treatment promotes functional regeneration to the brainstem, although a contribution from spared axons cannot be completely excluded.

In this study, central axons regenerated at an average rate of 0.2–0.4 mm/d, much slower than the rate of growth in lesioned white matter reported by Davies et al. (19). There may be several reasons for this difference. First, our preparation did not use a conditioning lesion to promote a more robust regenerative response. Second, chondroitin sulfate proteoglycans (CSPGs) produce a substantial barrier at the DR entry zone, dorsal horns, and dorsal columns near the site of DR crush (4). In our preparation, this CSPG-rich area would extend from C5 to T1, a distance of at least 1.5 cm through which axons might regenerate at a reduced rate. Finally, axon elongation slows at the border between the dorsal columns and the CN (19), which may contribute to the slower rate of overall growth. Despite these factors, this study demonstrates sustained axonal growth for several months, which would yield a substantial clinical benefit, particularly given the functionality and specificity of this regeneration.

Remarkably, ARTN promoted functional reinnervation of the correct areas in the brainstem without the addition of guidance molecules. Other studies have relied on gradients of neurotrophic factors to guide regenerating axons to correct brainstem regions, a technique that could equally lead axons astray if misplaced (5, 20). Identifying therapies that encourage proper guidance is paramount to the goal of long-distance regeneration (21, 22). With ARTN treatment, regeneration is topographically specific in the SC, with sensory axons reinnervating the correct regions of the dorsal horn (6). Similarly, the results of the present study demonstrate that regenerating axons reach the correct brainstem nucleus, suggesting that guidance cues persist in the adult CNS. Although targeting was not perfect, we hypothesize that ARTN treatment promotes regeneration over long distances, in part by stimulating growth in a targeted manner. The correct guidance of regenerating axons may be related to the fact that ARTN was administered systemically rather than directly into the SC or cerebrospinal fluid, which may overwhelm guidance cues. Second, ARTN was administered for only 12 d, yet led to continued axon growth. It is tempting to speculate that this may better mimic physiological growth signals, and that a temporal pattern of trophic support might be more important than continuous activation of growth pathways. Further experiments are needed to ascertain which intrinsic pathways are activated with ARTN treatment and to understand the manner by which ARTN results in a sustained regenerative response.

ARTN signals through the RET tyrosine kinase, an interaction that requires the binding of a nonsignaling coreceptor GFRα3 (23, 24). Previous studies have suggested that GFRα3 is expressed only rarely on myelinated sensory neurons (8, 9, 14), yet ARTN promotes robust regeneration of myelinated sensory axons (3, 6, 25). Given this inconsistency, we devised a method to quantify GFRα3 in specific populations of cells, and found similar expression in myelinated neurons and unmyelinated neurons. Given that RET is expressed on most sensory neurons (18), ARTN likely acts through the binding of GFRα3 and the RET tyrosine kinase to promote regeneration in both myelinated and unmyelinated neurons, although signaling through other binding partners is possible as well.

Several earlier studies reported an increase in the number of cells expressing GFRα3 after injury (3, 8, 14, 26). In contrast, we found decreased GFRα3 levels in DRG neurons shortly after DR crush that persisted for at least 12 d (Fig. 7). Our results differ from previous studies because many of those studies examined changes in GFRα3 expression after peripheral nerve injury rather than DR injury (8, 14, 26). Unlike DR crush, peripheral nerve injury up-regulates growth-promoting pathways. In one study using the DR crush model of injury, GFRα3$^+$ cells were counted, and a decrease in the number of myelinated GFRα3$^+$ neurons with a concomitant increase in unmyelinated GFRα3$^+$ neurons was observed (3). Here we found that GFRα3 expression decreases. This discrepancy may be attributed to differences in the sensitivity and resolution of these testing methodsis.

In summary, systemic ARTN treatment promotes targeted regeneration of adult sensory axons to the brainstem, a distance of >3 cm. Regenerating sensory axons reestablish synaptic connectivity with neurons in the CN, suggesting that guidance cues persist in the adult CNS, and adult neurons retain some intrinsic ability to follow these cues to appropriate target areas. Understanding the intrinsic pathways activated by ARTN can provide insight into new therapeutics to promote targeted and functional axon regeneration in the CNS.

## Materials and Methods

**DR Crush.** All experimental procedures were approved by the Tufts University School of Medicine's Institutional Animal Care and Use Committee and conformed to National Institutes of Health guidelines. Unilateral DR crushes were performed from C5 to T1 on male Sprague–Dawley rats (200–250 g) as described previously (2, 3, 6). Animals were treated with 1 mg/kg ARTN104,

3 mg/kg ARTN113, or saline vehicle for 2 wk after surgery (3). Animals with persistent sensory function after DR crush ($n = 3$ of 30) were excluded.

**Preparation and Purification of ARTN.** The 104-aa and 113-aa versions of rat ARTN were produced in *Escherichia coli* (12). A kinase receptor activation (KIRA) ELISA determined that the preparations were indistinguishable in their ability to promote RET phosphorylation with $EC_{50}$ values of 1 nM.

**Neuroanatomy.** To trace the central projections of sensory axons, rats were anesthetized, the radial nerve was exposed, 4 μL of a 1% solution of 10,000-molecular weight mini-Ruby dextran (Life Technologies) in PBS was injected using a Hamilton syringe, and muscle and skin were closed. After 7 d, rats were perfused with 4% paraformaldehyde in PBS, and the SC and brainstem were removed. Then 25-μm cryostat sections were imaged with a Leica SP2 confocal microscope; 10- to 15-μm Z-stacks were obtained using steps of 0.8 μm and fixed exposure settings. Puncta were quantified using ImageJ by a researcher blinded to the identity and treatment of the animal.

**Electrophysiology.** Anesthetized animals received 1 mg/kg of dexamethasone before brainstem exposure. Median and ulnar nerves were stimulated with square 50-μs, 2-V pulses delivered at 5 Hz using a digital stimulus isolator (model 2300; A-M Systems) driven by custom LabVIEW software (National Instruments). Recordings were made using a 1 × 16-channel microelectrode (NeuroNexus), with recording locations spaced vertically at 100-μm intervals, from three recording sites in the CN bilaterally. The three recording sites were chosen based on our extensive mapping of maximum responses in the CN of normal animals.

Single responses were recorded with a 16-channel amplifier (model 3600; A-M Systems), filtered (0.3 Hz–10 kHz), and digitized (16-bit, 20-kHz sampling rate) using custom LabVIEW software. Fifty traces were averaged and stored for analysis offline at each of the 16 locations at each site. The response (average, 0.5–6.5 ms) was used as the physiological measure of the summed short-latency response at each location. At each site, the largest response of the 16 recordings was selected, and the largest response of the three recording sites for each experimental animal was chosen. SC recordings were made as described previously (3). The extent of regeneration was calculated independently for each animal as the ratio of the maximum response on the regenerated side to that on the unlesioned side.

**FACS and Quantification of GFRα3 Expression.** To label distinct populations of DRG neurons, a mixture of CTB-488 and WGA-647 (Life Technologies) was injected into the brachial nerves at 2 d before DRG harvesting. Suspensions of dissociated sensory neurons were made using a protocol modified from Malin et al. (27), combining brachial DRGs from 12 rats to provide sufficient material for analysis. The samples were filtered with a 40-μL Flowmi cell strainer (Bel-Art Products). CTB-488$^+$ and WGA-647$^+$ cells were sorted into tubes containing media supplemented with 200 mM ascorbic acid using a Beckman Coulter Moflo Legacy cell sorter. FACS was performed in triplicate.

cDNA was made with the SuperScript III CellsDirect cDNA synthesis kit (Life Technologies) and a mixture of Oligo$(dT)_{20}$ and random primers. qPCR was performed using the appropriate primer pair (Table S1) in a SYBR Green Master Mix (Applied Biosystems). Samples were run in triplicate, with each amplification including reactions without template as negative controls. Relative fold changes were calculated using the ΔΔCt method with Pfaffl correction for PCR amplification efficiency (28), using both *GAPDH* and *HPRT* as reference genes (29).

**Immunohistochemistry.** The 25-μm cryostat sections were processed using goat anti-GFRα3 (1:400; R&D Biosystems), rabbit anti-NeuN (1:200; Abcam), mouse anti-NF200 (1:1,000; Sigma-Aldrich), and mouse anti-CGRP (1:1,000; Sigma-Aldrich). Slides were incubated in primary antibody diluted in blocking solution (2% normal horse serum and 0.2% Triton X-100 in PBS) at 4 °C for 18 h. Primary antibody binding was visualized with chicken anti-goat, donkey anti-rabbit, or rabbit anti-mouse secondary antibodies conjugated to Alexa Fluor 488 or Alexa Fluor 568. Cells were counted using ImageJ. To verify GFRα3 antibody specificity, tissue from two GFRα3$^{-/-}$ mice and two GFRα3$^{+/-}$ littermate controls was generously provided by the H. Enomoto laboratory (15). GFRα3 protein expression in DRG neurons was quantified with a mean pixel intensity of GFRα3 immunostaining in NeuN$^+$ cells using ImageJ. At least 250 cells were counted from three different animals at each time point. Boxplots depict intensity levels for all cells counted, with outliers plotted individually (30).

**Statistical Analysis.** All statistical analyses were performed using the Student *t* test or ANOVA, with Bonferroni's post hoc correction for multiple analyses when appropriate. Results were considered significant for tests with a $P$ value $< 0.05$.

**ACKNOWLEDGMENTS.** We thank Bang-Jian Gong and Tony Rossomando for their purification of ARTN, Paul Carmillo for his evaluation of samples in the KIRA ELISA, Pamela Harvey for her instrumental contributions to the pilot experiments in this study, and Stephen Kwok for his helpful technical contributions to the paper. Rat ARTN was provided by Biogen Idec, Inc. This work was supported by the National Institutes of Health (Grant NS064494, to E.F.), a gift from the Murray Winston Foundation, and a grant from the Craig H. Nielsen Foundation.

1. Smith GM, Falone AE, Frank E (2012) Sensory axon regeneration: Rebuilding functional connections in the spinal cord. *Trends Neurosci* 35(3):156–163.
2. Harvey PA, Lee DH, Qian F, Weinreb PH, Frank E (2009) Blockade of Nogo receptor ligands promotes functional regeneration of sensory axons after dorsal root crush. *J Neurosci* 29(19):6285–6295.
3. Wang R, et al. (2008) Persistent restoration of sensory function by immediate or delayed systemic artemin after dorsal root injury. *Nat Neurosci* 11(4):488–496.
4. Ramer MS, Priestley JV, McMahon SB (2000) Functional regeneration of sensory axons into the adult spinal cord. *Nature* 403(6767):312–316.
5. Alto LT, et al. (2009) Chemotropic guidance facilitates axonal regeneration and synapse formation after spinal cord injury. *Nat Neurosci* 12(9):1106–1113.
6. Harvey P, Gong B, Rossomando AJ, Frank E (2010) Topographically specific regeneration of sensory axons in the spinal cord. *Proc Natl Acad Sci USA* 107(25):11585–11590.
7. Baloh RH, et al. (1998) GFRalpha3 is an orphan member of the GDNF/neurturin/persephin receptor family. *Proc Natl Acad Sci USA* 95(10):5801–5806.
8. Keast JR, Forrest SL, Osborne PB (2010) Sciatic nerve injury in adult rats causes distinct changes in the central projections of sensory neurons expressing different glial cell line-derived neurotrophic factor family receptors. *J Comp Neurol* 518(15):3024–3045.
9. Orozco OE, Walus L, Sah DWY, Pepinsky RB, Sanicola M (2001) GFRalpha3 is expressed predominantly in nociceptive sensory neurons. *Eur J Neurosci* 13(11):2177–2182.
10. Fraher JP (2000) The transitional zone and CNS regeneration. *J Anat* 196(Pt 2):161–182.
11. Di Maio A, et al. (2011) In vivo imaging of dorsal root regeneration: Rapid immobilization and presynaptic differentiation at the CNS/PNS border. *J Neurosci* 31(12):4569–4582.
12. Silvian L, et al. (2006) Artemin crystal structure reveals insights into heparan sulfate binding. *Biochemistry* 45(22):6801–6812.
13. Naveilhan P, et al. (1998) Expression and regulation of GFRalpha3, a glial cell line-derived neurotrophic factor family receptor. *Proc Natl Acad Sci USA* 95(3):1295–1300.
14. Bennett DLH, et al. (2000) The glial cell line-derived neurotrophic factor family receptor components are differentially regulated within sensory neurons after nerve injury. *J Neurosci* 20(1):427–437.
15. Honma Y, et al. (2002) Artemin is a vascular-derived neurotropic factor for developing sympathetic neurons. *Neuron* 35(2):267–282.
16. LaMotte CC, Kapadia SE, Shapiro CM (1991) Central projections of the sciatic, saphenous, median, and ulnar nerves of the rat demonstrated by transganglionic transport of choleragenoid-HRP (B-HRP) and wheat germ agglutinin-HRP (WGA-HRP). *J Comp Neurol* 311(4):546–562.
17. Shehab SA, Hughes DI (2011) Simultaneous identification of unmyelinated and myelinated primary somatic afferents by co-injection of isolectin B4 and Cholera toxin subunit B into the sciatic nerve of the rat. *J Neurosci Methods* 198(2):213–221.
18. Luo W, et al. (2007) A hierarchical NGF signaling cascade controls Ret-dependent and Ret-independent events during development of nonpeptidergic DRG neurons. *Neuron* 54(5):739–754.
19. Davies SJ, Goucher DR, Doller C, Silver J (1999) Robust regeneration of adult sensory axons in degenerating white matter of the adult rat spinal cord. *J Neurosci* 19(14):5810–5822.
20. Bonner JF, et al. (2011) Grafted neural progenitors integrate and restore synaptic connectivity across the injured spinal cord. *J Neurosci* 31(12):4675–4686.
21. Pernet V, et al. (2013) Long-distance axonal regeneration induced by CNTF gene transfer is impaired by axonal misguidance in the injured adult optic nerve. *Neurobiol Dis* 51:202–213.
22. Luo X, et al. (2013) Three-dimensional evaluation of retinal ganglion cell axon regeneration and pathfinding in whole mouse tissue after injury. *Exp Neurol* 247:653–662.
23. Baloh RH, et al. (1998) Artemin, a novel member of the GDNF ligand family, supports peripheral and central neurons and signals through the GFRalpha3-RET receptor complex. *Neuron* 21(6):1291–1302.
24. Wang X, Baloh RH, Milbrandt J, Garcia KC (2006) Structure of artemin complexed with its receptor GFRalpha3: Convergent recognition of glial cell line-derived neurotrophic factors. *Structure* 14(6):1083–1092.
25. Wang R, et al. (2014) Artemin-induced functional recovery and reinnervation after partial nerve injury. *Pain* 155(3):476–484.
26. Wang T, et al. (2011) Phenotypic switching of nonpeptidergic cutaneous sensory neurons following peripheral nerve injury. *PLoS ONE* 6(12):e28908.
27. Malin SA, Davis BM, Molliver DC (2007) Production of dissociated sensory neuron cultures and considerations for their use in studying neuronal function and plasticity. *Nat Protoc* 2(1):152–160.
28. Pfaffl MW (2001) A new mathematical model for relative quantification in real-time RT-PCR. *Nucleic Acids Res* 29(9):e45.
29. Piller N, Decosterd I, Suter MR (2013) Reverse-transcription quantitative real-time polymerase chain reaction reference genes in the spared nerve injury model of neuropathic pain: Validation and literature search. *BMC Res Notes* 6:266.
30. Krzywinski M, Altman N (2014) Visualizing samples with box plots. *Nat Methods* 11(2):119–120.